ADVANCED HEALTHCARE MATERIALS
www.advhealthmat.de

Patterned Three-Dimensional Encapsulation of Embryonic Stem Cells using Dielectrophoresis and Stereolithography

*Piyush Bajaj, Daniel Marchwiany, Carlos Duarte, and Rashid Bashir**

Controlling the assembly of cells in three dimensions is very important for engineering functional tissues, drug screening, probing cell-cell/cell-matrix interactions, and studying the emergent behavior of cellular systems. Although the current methods of cell encapsulation in hydrogels can distribute them in three dimensions, these methods typically lack spatial control of multi-cellular organization and do not allow for the possibility of cell-cell contacts as seen for the native tissue. Here, we report the integration of dielectrophoresis (DEP) with stereolithography (SL) apparatus for the spatial patterning of cells on custom made gold micro-electrodes. Afterwards, they are encapsulated in poly (ethylene glycol) diacrylate (PEGDA) hydrogels of different stiffnesses. This technique can mimic the in vivo microscale tissue architecture, where the cells have a high degree of three dimensional (3D) spatial control. As a proof of concept, we show the patterning and encapsulation of mouse embryonic stem cells (mESCs) and C2C12 skeletal muscle myoblasts. mESCs show high viability in both the DEP (91.79% ± 1.4%) and the no DEP (94.27% ± 0.5%) hydrogel samples. Furthermore, we also show the patterning of mouse embryoid bodies (mEBs) and C2C12 spheroids in the hydrogels, and verify their viability. This robust and flexible in vitro platform can enable various applications in stem cell differentiation and tissue engineering by mimicking elements of the native 3D in vivo cellular micro-environment.

1. Introduction

Native tissues are composed of a complex 3D micro-environment where the cells are presented with a myriad of different cues including mechanical, geometrical, chemical, and electrical. These cues are responsible for guiding the cells through differentiation, proliferation, and migration.[1–6] It has been a long-standing goal of researchers to mimic this complex 3D architecture in vitro, towards the construction of a cellular niche for recapitulating the in vivo cues.[7–10] In order to achieve mimicry of the native tissue, spatially organized 3D co-cultures of multiple cell types are required to recapitulate the cellular interactions.[11] However, difficulties in controlling the spatial arrangement of cells, in preserving cell functionality, and in maintaining the physical properties of the 3D matrix have prevented the reconstruction of the native tissue in vitro.

Hydrogels have attracted much attention recently because of their use in a variety of biomedical applications such as drug delivery, wound management and tissue engineering.[12–15] Many studies have used different techniques like solvent casting,[16] freeze drying,[17] gas foaming,[18] electrospinning,[19] and SL[20] for constructing the complex 3D architecture found in the body using hydrogels. Among these techniques, SL offers several unique advantages like multi-cell, multi-material fabrication and the capability to encapsulate cells during the process of structure fabrication.[21] Also, unlike other photo-polymerization techniques which require a physical mask, SL is a maskless computer aided design (CAD) based rapid prototyping (RP) technology. Such merits of SL apparatus make it a great technology for tissue engineering applications and regenerative medicine.[22] However, micro-scale tissue organization, a hallmark of in vivo tissues, cannot be achieved by conventional SL apparatus due to limitations in the beam width. Commercially available lasers typically have beam widths in the range of few hundred microns, which is much larger than size of single cells.[23]

DEP has been widely used by researchers over the past few decades for manipulating biological entities. DEP is advantageous for creating massively parallel cellular patterns. This coupled to the fact that mammalian cells can withstand high frequency electrical signals for short bursts of time, DEP emerges as a very lucrative patterning technique for mammalian cells.[24] However, one of the limiting factors is that the DEP force is temporary and hence the cells are free to move around once the

P. Bajaj, R. Bashir
Department of Bioengineering
University of Illinois at Urbana-Champaign
Urbana, IL 61801, USA
Email: rbashir@illinois.edu
P. Bajaj, D. Marchwiany, C. Duarte, R. Bashir
Micro and Nanotechnology Laboratory
University of Illinois at Urbana-Champaign
Urbana, IL 61801, USA
D. Marchwiany
Department of Molecular and Cellular Biology
University of Illinois at Urbana-Champaign
Urbana, IL 61801, USA
C. Duarte, R. Bashir
Department of Electrical and Computer Engineering
University of Illinois at Urbana-Champaign
Urbana, IL 61801, USA

DOI: 10.1002/adhm.201200318

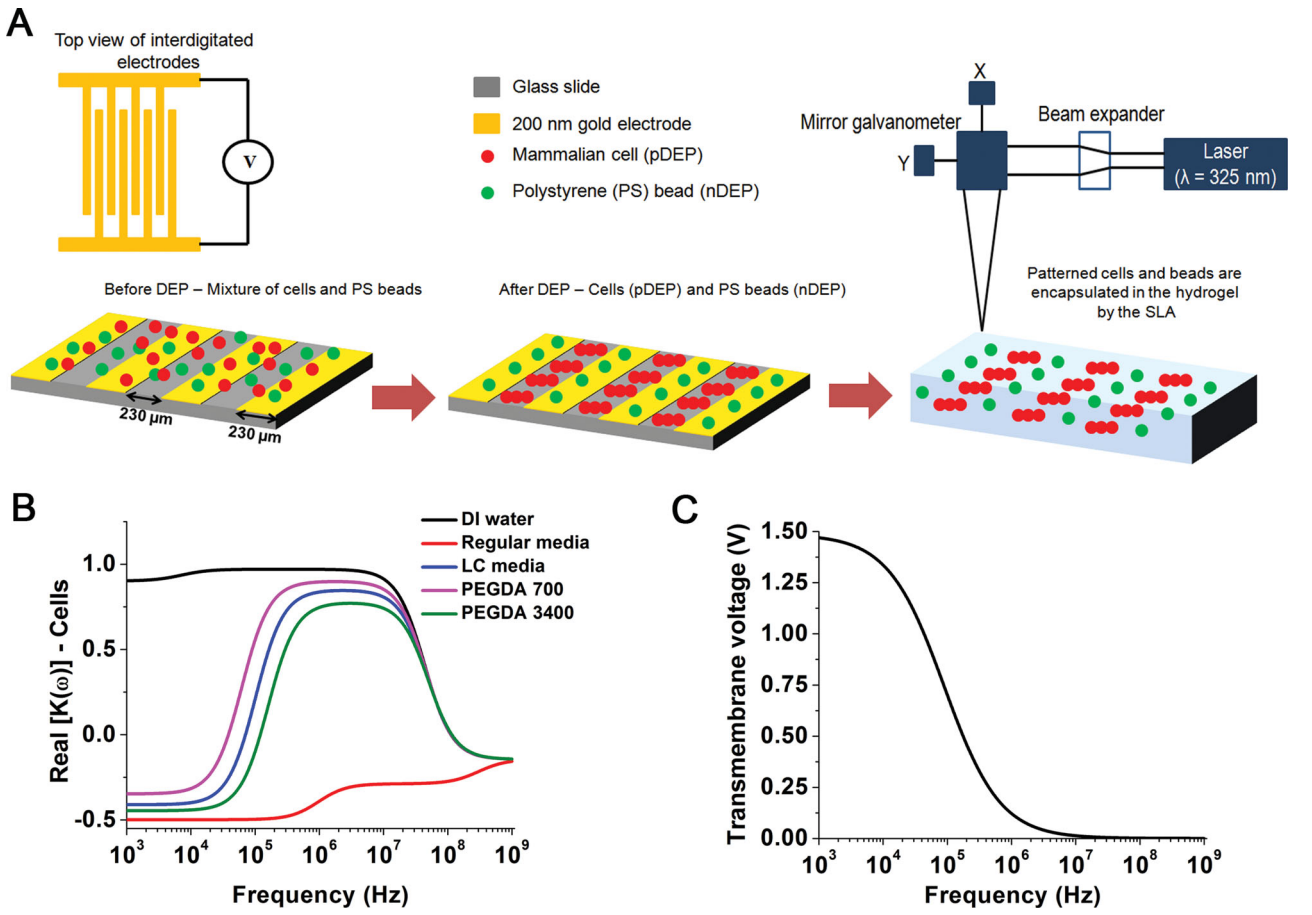

Figure 1. Fabrication of spatially patterned 3D hydrogel constructs. (A) Schematic showing the overall process of creating 3D spatially patterned hydrogel constructs. A mixture of cells and PS beads is first introduced on the glass slide with patterned gold electrodes. After this the electrodes are energized with a 10 V_{pp} (3.535 V_{rms}) 1-10 MHz signal which leads to pDEP patterning of the cells and nDEP patterning of the PS beads. The SL apparatus then polymerizes the PEGDA polymer and patterned cells and beads get encapsulated in the 3D hydrogel. (B) Real part of the CM factor for mammalian cells in the different fluids used for DEP patterning. Between 1-10 MHz, mammalian cells always undergo pDEP for the two different polymers (PEGDA 700 and 3400) used in this study. (C) TMV of the cells as a function of applied frequency.

force is removed. Therefore, DEP needs to be combined with other immobilization techniques for long term patterned cell culture.[25–27]

In this study, we combine the merits of SL apparatus and DEP together to create hydrogels of physiologically relevant stiffnesses with micro-scale organization as seen for in vivo tissues. We show the patterning and encapsulation of mouse embryonic stem cells (mESCs) and C2C12 skeletal muscle myoblasts in the hydrogels. However, as cell clusters (spheroids of cells) of different sizes can locally alter the cellular micro-environment via differential gene expression,[28] we also show the patterning of mouse embryoid bodies (mEBs) and C2C12 spheroids in the hydrogels. Previous studies have only focused on patterning individual cells via DEP forces in hydrogels.[29,30] This platform can thus be used to create hydrogels with micro-scale tissue architecture and enable applications in tissue engineering, regenerative medicine, and stem cell differentiation.

2. Results and Discussion

2.1. Process for Patterning Mammalian Cells in 3D Hydrogels

Figure 1A shows the schematic of the overall process of simultaneous patterning and encapsulation of mammalian cells and polystyrene (PS) beads on gold micro-electrodes. The scheme for fabricating gold electrodes can be seen in figure S1 (Supporting Information). Cells and beads were first patterned by means of DEP forces to achieve spatial patterning. They were then encapsulated in the hydrogel by the SL apparatus. In order to achieve efficient DEP patterning, the DEP liquid medium needs to have low conductivity and low viscosity.[31] Low conductivity minimizes Joule heating while low viscosity decreases the drag force and patterning time. **Table 1** shows the properties of the DEP liquid used in this study and some standard solutions. Albrecht et al., derived an equation which showed that the patterning time scales linearly with the viscosity of the

DOI: 10.1002/adhm.201200318

Table 1. Electrical and viscous properties of the fluids.

Liquid used for DEP patterning	Concentration [%]	Electrical conductivity [mS m^{-1}]	Viscosity [cP]
DI water	100	0.105	1.04
Cell culture medium	100	1504	1.11
Low conductivity (LC) medium	100	23.55	1.31
PEGDA 700 in LC medium	10	15.78	2.05
	15	13.16	2.62
	20	10.64	3.46
PEGDA 3400 in LC medium	10	36.9	3.69
	15	39.9	5.83
	20	41.2	9.97

medium. Therefore, lower the viscosity of the medium faster the patterning time.[31] Although, the viscosity of regular cell culture medium (RM) is low (1.11 cP), it has a relatively high electrical conductivity, 1504 mS m^{-1}. As a result, RM will cause excessive Joule heating which could be detrimental to the viability of cells.[32] Therefore, a different medium was used for patterning of cells and beads. This new medium had both low viscosity (1.31 cP) and low conductivity (23.55 mS m^{-1}). It not only allowed efficient DEP patterning but also maintained very high cell viability (Supporting Information, Figure S2). Two different molecular weight (M_w) PEGDA polymers, 700 and 3400, at three different concentrations (10%, 15% and 20%) were used to form hydrogels. The low conductivity medium (LCM) was used as the solvent for the polymers. By varying the M_w and the concentration of the polymer, we were able to obtain hydrogels of physiologically relevant stiffnesses.[1,20,33] For both the polymers used in the study, the viscosity increases with an increase in the polymer concentration. As a result of this, the fastest patterning time (τ) was achieved in 10% PEGDA 700 ($\tau <$ 10 s), which is the lowest viscosity polymer. It took close to 240 s to pattern cells in 20% PEGDA 3400, the highest viscosity polymer. Also higher voltages were required to pattern cells in this polymer. Unless otherwise specified, all the results presented in this study were obtained in 15% PEGDA 3400 ($\tau \sim 90$ s). mESCs show a good viability in LCM for holding time up 30 minutes (Supporting Information, Figure S2). Given the patterning time of cells in the different solutions, multiple hydrogel constructs could be easily fabricated while maintaining good viability. As the same polymer solution was used for fabrication of multiple constructs, batch-to-batch variability in terms of material properties was eliminated. The size of the assembly that could be patterned using DEP is dependent on the area of electrodes, the spacing of electrodes, and the area that could be polymerized by the SL apparatus. It is independent of the liquid medium used for patterning. In this study, cells were patterned and encapsulated in a 10 mm × 10 mm area of the hydrogel. Thus this platform can be used for constructing very large arrays of micro-scale cellular patterns in three dimensions.

Figure 1B shows the real part of the Clausius Mossotti (CM, K(ω)) factor for mammalian cells in the different liquid medium. It can be seen that for the polymers used in the study, the cells will experience both negative DEP (nDEP) and positive DEP (pDEP) depending on the frequency. Specifically, for PEGDA 3400, at frequencies lower than 0.12 MHz or at frequencies higher than 115 MHz, cells will experience nDEP. Between these frequency ranges, the cells experience pDEP. Since, it is well documented that patterning via pDEP is faster than nDEP, pDEP was used for patterning of cells.[31] Furthermore, CM factor which also determines the relative DEP force is also larger in the pDEP regime. Therefore, for PEGDA 700 and PEGDA 3400, a frequency range of 1-10 MHz was chosen. This maximized the CM factor and hence the relative DEP force experienced by the cells. At the same frequency range, the PS beads experienced nDEP (Supporting Information, Figure S3 D).

Mammalian cells have a large differential of ions between its interior and exterior leading to the development of a resting membrane potential. The maintenance of this resting membrane potential is of utmost importance for the proper functioning of the cellular activities. When an alternating sinusoidal electric field is applied to a cell, this new field gets superimposed to the resting membrane potential. If the resultant resulting membrane potential is sufficiently high, it might lead to an asymmetric breakdown of the cellular membrane causing cell death.[34] Irreversible cellular electroporation occurs at field strengths of 1-1.3 kV cm^{-1}.[35] This means that a potential difference of approximately 1 V can be potentially lethal for a cell of diameter 10 μm. Figure 1C shows the transmembrane voltage (TMV) in the cell as a function of the applied electric field from 1 kHz to 1 GHz. For the frequency range used for patterning of cells in the polymers (1–10 MHz), the transmembrane voltage is around 0.12–0.013 V respectively. Since, this value is much smaller than the threshold voltage of 1 V, the cells will not undergo irreversible electroporation as a result of dielectrophoretic manipulation. Supporting Information discusses the parameters used for calculation of TMV in detail. Since, both the CM factor and the TMV are optimized between 1–10 MHz for the polymers, this range was chosen for patterning of cells via DEP.

2.2. Patterning mESCs, C2C12 Cells in 3D Hydrogels

Figures 2A–C shows the encapsulated C2C12 cells and mESCs in 15% and 20% PEGDA 700 hydrogels. Highly uniform arrays of cells and beads can be seen encapsulated in the hydrogel after polymerization. This indicates that DEP forces can be used for manipulating cells in the polymers. Before patterning the cells in the polymer, their viability was checked in the LCM. Figure S2 (Supporting Information) shows that mESCs show a high viability after being suspended in a LCM for 30 minutes and this was not statistically different ($p < 0.05$) from that of the cells in RM. Figures 2A,B shows that C2C12 cells (red) undergo pDEP and PS beads (green) undergo nDEP at 10 MHz in 15% PEGDA 700. Figure 2C shows the same for mESCs (red) in 20% PEGDA 700. Lee et al., showed that incorporation of hydrophobic nanoparticles can introduce network defects in the hydrogel while minimally affecting its mechanical and viscous properties.[36] Therefore, controlling the position of hydrophobic PS beads via DEP forces can be used to create network defects at regular spatial locations in the hydrogel. This can

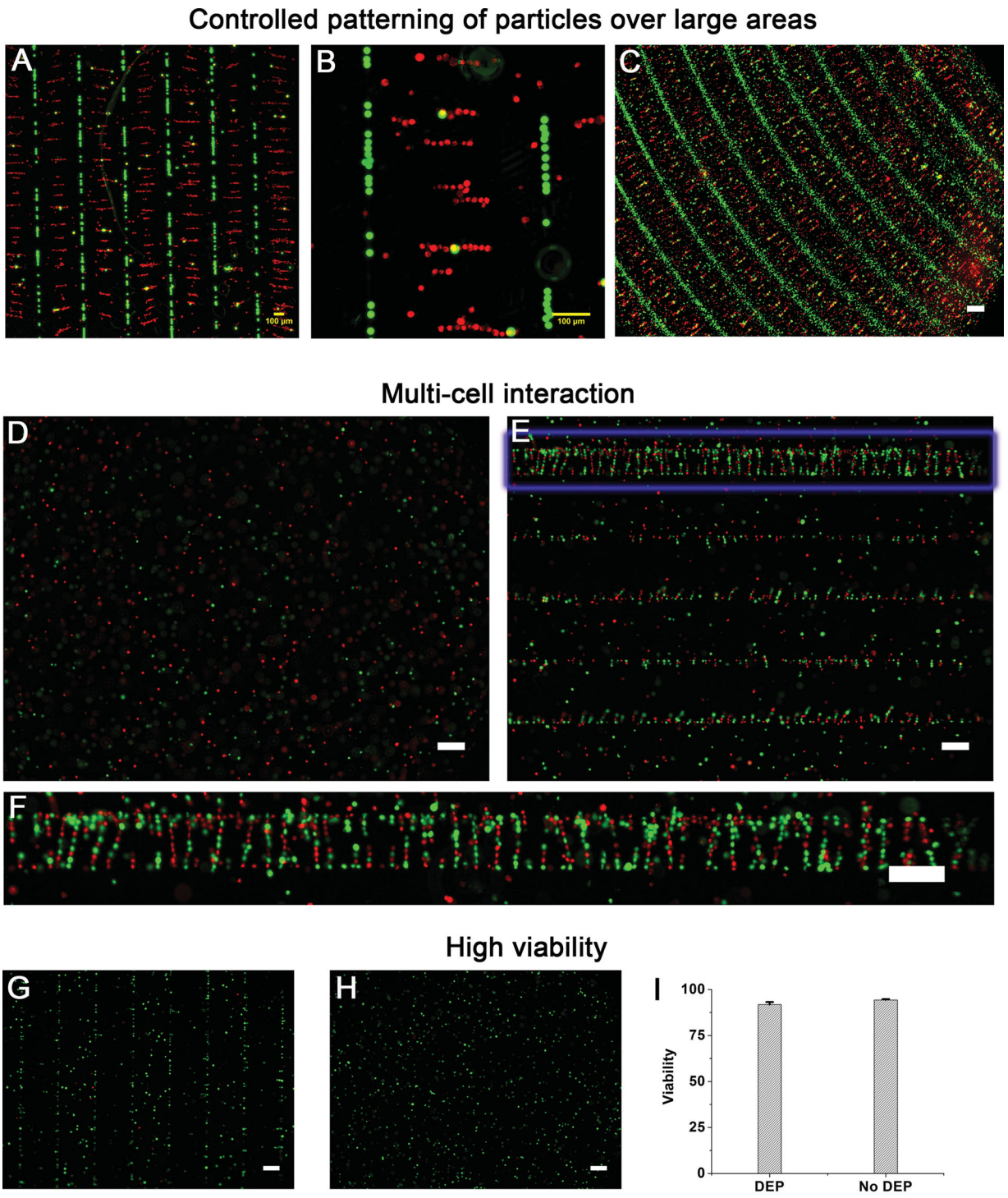

Figure 2. Multi-cell patterning and encapsulation in different stiffness hydrogels by using DEP and SL apparatus (A-C) This platform can be used to create large scale patterns of mammalian cells in 3D hydrogels. (A) C2C12 cells (red) (pDEP) and PS beads (green) (nDEP) in 15% PEGDA 700 (Scale bar = 100 µm) (B) Zoomed image of (A) (Scale bar = 100 µm) (C) mESCs (red) (pDEP) and PS beads (green) (nDEP) in 20% PEGDA 700 (Scale bar = 200 µm) by using spiral electrodes. (D-F) mESCs with two different colored dyes (red and green) were encapsulated in 15% PEGDA 3400. (D) Without DEP (Scale bar = 100 µm). (E) With DEP (Scale bar = 100 µm). (F) Zoomed image of the highlighted blue box in (E) clearly showing cell-cell interactions in the hydrogel (Scale bar = 100 µm). (G-I) Demonstrates that high cell viability can be achieved using this platform. (G) Live/dead assay at day 0 with DEP (Scale bar = 100 µm). (H) Live/dead assay at day 0 without DEP (Scale bar = 100 µm). (I) Graph showing the viability of cells with and without DEP. Green indicates live cells and red shows dead cells for (G-I) (n = 5). Viability was calculated by counting the red cells, green cells and taking the ratio of green cells to the total number (green + red) of cells.

Adv. Healthcare Mater. **2012**,
DOI: 10.1002/adhm.201200318

improve the permeability of compounds through the hydrogel and thereby improve their viability.

Figures 2D–F shows the encapsulation of mESCs with two different colored dyes (green and red) in 15% PEGDA 3400. By encapsulation of multiple types of cells using conventional SL, the two different types of cells are generally present with minimal cell-cell contacts in the hydrogel (Figure 2D). While these co-culture studies can be very useful for studying paracrine signaling,[21] cell-cell contacts which are responsible for fate decisions by embryonic stem cells cannot be studied using this approach.[37] However, as seen in Figures 2E and F, DEP allows cell-cell contacts by formation of cellular pearl chains. These pearl chains can be used for studying the fate decisions by stem cells. Numerous studies have demonstrated the role of cellular co-culture for determining the fate of ESCs.[38,39] This combined DEP-SL apparatus platform will enable the study of multiple cell interactions via cell-cell contacts in 3D and can open new doors in stem cell biology.

Figure 2G, H shows the image of a live/dead assay for mESCs with and without DEP on day 0 in 15% PEGDA 3400. It can be seen from these fluorescent images that most of the cells survive patterning via DEP and SL encapsulation. Figure 2I quantifies the viability of cells with and without DEP. The cells which were aligned in the hydrogel with DEP show a viability of 91.79 ± 1.4% while those which were not subjected to DEP show a slightly higher viability of 94.27 ± 0.5%. Thus these studies show that our combined platform can be used for studying multi-cell interactions in 3D hydrogels while maintaining their viability.

2.3. Formation and Characterization of mEBs

mEBs are 3D aggregates of mESCs and serve as an excellent model for studying the controlled differentiation of mESCs. As previously shown, the differentiation of cells in the EBs is extremely sensitive to a variety of factors including the size (density of cells) of the EB. Larger EBs (~ 450 μm) promote cardiogenesis while smaller EBs (~ 150 μm) promote endothelial differentiation.[28] We formed large number of uniform sized EBs using AggreWell plates. Desired numbers of cells were seeded, centrifuged, and incubated in the plates. After 24 hours of incubation, highly uniform EBs were seen in the microwells of the plate. **Figure 3**A shows the different initial seeding densities of mESCs in the plates at 0 hours and the resultant EBs that formed after 24 hours in one of the microwells of the plate. Each of these plates contain anywhere from 9600 to 28200 microwells. Hence, a large number of uniformly sized EBs can be rapidly obtained. Figure 3B(i) is an SEM showing the uniformity of the EBs obtained from these plates. Figure 3B(ii) shows an individual EB while Figure 3B(iii) shows the close-up of an individual EB. These SEMs show that large number of highly uniform EBs can be obtained using AggreWell plates. Figure 3C shows the area of EBs as a function of the initial seeding density of the cells. Interestingly, the area of the EB does not double by doubling the initial cell seeding density. This suggests that the packing properties of cells in the EBs are a density dependent phenomenon. Figure 3D shows the theoretical and the measured volume of the EBs as a function of the initial seeding density of cells. It can be seen that the theoretical volume matches closely to the calculated volume of the EBs. The inset of the figure shows the radius of the EB as a function of the initial seeding density. Both the theoretical and measured radius show good match as well. A 250 cell EB measured 68 μm while this radius increased to only 110 μm by increasing the initial cell seeding density to 2000 cells. Therefore, larger mEBs show a higher packing density which can be seen in Figure 3E. This could be possible because of differences in the E-cadherin expression in the EBs. Different levels in E-cadherin expression have been reported for EBs of different sizes and different time points.[28] 1000 cell EB shows the highest packing density of approximately 425 000 cells mm^{-3}. Also, the same EB shows the best packing efficiency which is the ratio of measured volume to the theoretical volume. Future studies can explore the effect of packing density and packing efficiency on the differentiation potential of mEBs. In addition, to further understand the packing properties of the EBs, they can be labeled for E-cadherin which will show cell-cell contacts in the EBs.[37]

2.4. Patterning of Cell Clusters in 3D Hydrogels

After the successful formation of mEBs (or spheroids of C2C12 cells, for characterization of C2C12 spheroids, see Figure S4 in the Supporting Information), we show the patterning and encapsulation of these cell clusters in the hydrogels as well. **Figure 4**A i, ii, show the images of 500 cell C2C12 spheroids with and without DEP in 15% PEGDA 700 respectively. The spheroids have been labeled with a red colored cell tracker dye. For the convenience of the reader, we have drawn the approximate locations of the underlying electrodes (Figure 4Ai) for the DEP sample. It can be seen that the spheroids of C2C12 cells undergo pDEP in 15% PEGDA 700 at 1 MHz. Most of the spheroids can be seen touching the edges of the electrodes (electric field maxima) and trying to form pearl chains, a characteristic of pDEP. Supporting Information, Figure S5 shows the patterning of C2C12 spheroids via DEP in 15% PEGDA 700 on a printed circuit board. Presence of multiple pearl chains of C2C12 spheroids can be clearly seen in these images further confirming that cell spheroids undergo pDEP. The inset of Figure 4A shows the fast Fourier transform (FFT) of the raw grayscale image (without the electrodes) which was used to check the alignment of the spheroids.[40,41] Figure 4B shows the FFT alignment plot for the spheroids encapsulated in 15% PEGDA 700 hydrogels. The FFT alignment plot shows a major peak at 180° (peak FFT = 0.103) for the sample which underwent DEP manipulation. Since FFT is a symmetric function, two other peaks can also be seen at 0° and 360° respectively. The sample with no DEP shows two very small peaks at 90° and 270° (peak FFT = 0.031) with very small signal to noise ratio of 1.47. If a circular mask was applied to this image, peaks were also seen at 0°, 90°, 180°, 270°, and 360°. Therefore, this sample does not show a net alignment for the spheroids. See Supporting Information for explanation of edge effects in alignment quantification and ways to remove them. In this study, all the alignment quantification has been performed without using a circular mask. The height and the overall shape of the

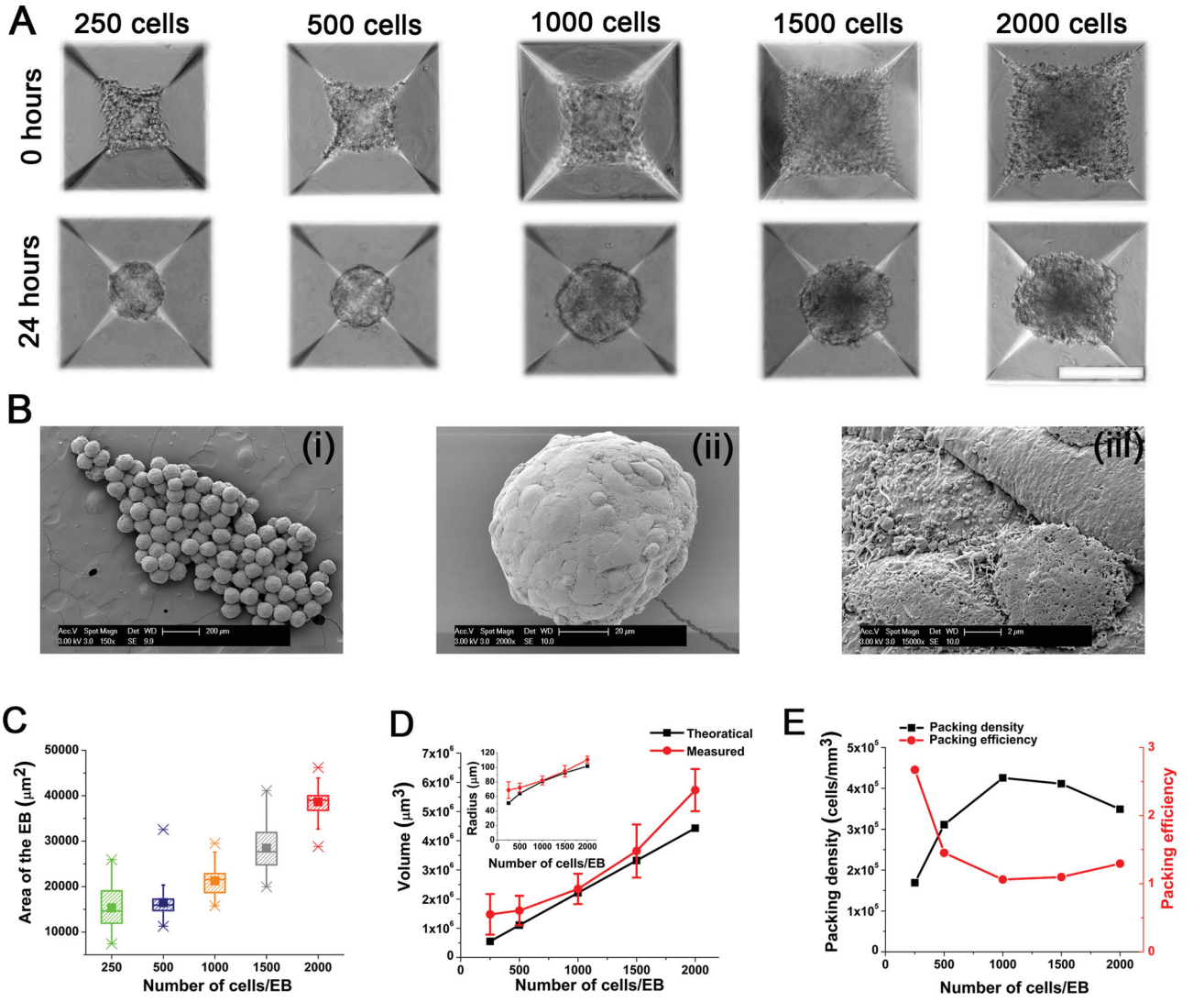

Figure 3. Characterization of EBs of mESCs. (A) Different densities of cells (250, 500, 1000, 1500, and 2000) seeded in AggreWell plates at 0 hours and after 24 hours (Scale bar = 200 μm). (B) SEMs of a 1000 cell mEBs at different resolution (i) Shows the uniformity of the EBs obtained from the AggreWell plates (Scale bar = 200 μm). (ii) An individual EB (Scale bar = 20 μm). (iii) Close up of the EB (Scale bar = 2 μm). (C) The area of the EBs as a function of the initial seeding density. (D) The volume of the EBs as a function of the initial seeding density. The inset shows the radius for the same. (E) Packing density and packing efficiency of the EBs as a function of the initial seeding density. Packing efficiency was calculated by dividing the actual volume by theoretical volume, $n > 50$ EBs for (C-E).

peaks represent the degree of alignment in the original image. A high and narrow peak indicates a more uniform degree of alignment while a broad peak indicates that more than one axis of alignment may be present. A completely random alignment is shown by no discernible peak in the alignment plot or by the presence of peaks at multiple peaks 0°, 90°, 180°, 270°, and 360° in the same alignment plot.[42] For an excellent discussion on the technique the reader is recommended to look at Ayres et al.[42] Directional basis in a material develops at 0.05 units or higher.[41–43] Hence, DEP can be used to align spheroids of cells (cellular aggregates or clusters) in the hydrogels as well. To our knowledge, this is the first study showing the patterning of spheroids in 3D hydrogels via DEP.

Figure 4C shows the live/dead images of mEBs (500 cell spheroids of mESCs) in 15% PEGDA 3400 for days 1, 3 and 5. From these images, it can be seen that mEBs easily survive this combined process of DEP-SL apparatus and show a good viability. Figure 4D show FFT alignment plots for the images shown in Figure 4C. These alignment plots show that mEBs that were subjected to DEP were patterned in the hydrogel as evidenced by the high, narrow peak and the corresponding high peak FFT values. The hydrogels that were not subjected DEP show more than one degree of alignment and relatively low peak FFT values, indicative of no net alignment. Figure 4E shows the viability of mEBs in the hydrogel. There is no statistical difference in viability for the samples that were subjected to DEP and no DEP for days 1 ($p = 0.703$), 3 ($p = 0.443$) and 5 ($p = 0.096$). Viability in this plot is the ratio of integrated density (area X mean gray value) of FITC (live cells) filter to TRITC (dead cells) filter. Even after five days in the hydrogel both the

DOI: 10.1002/adhm.201200318

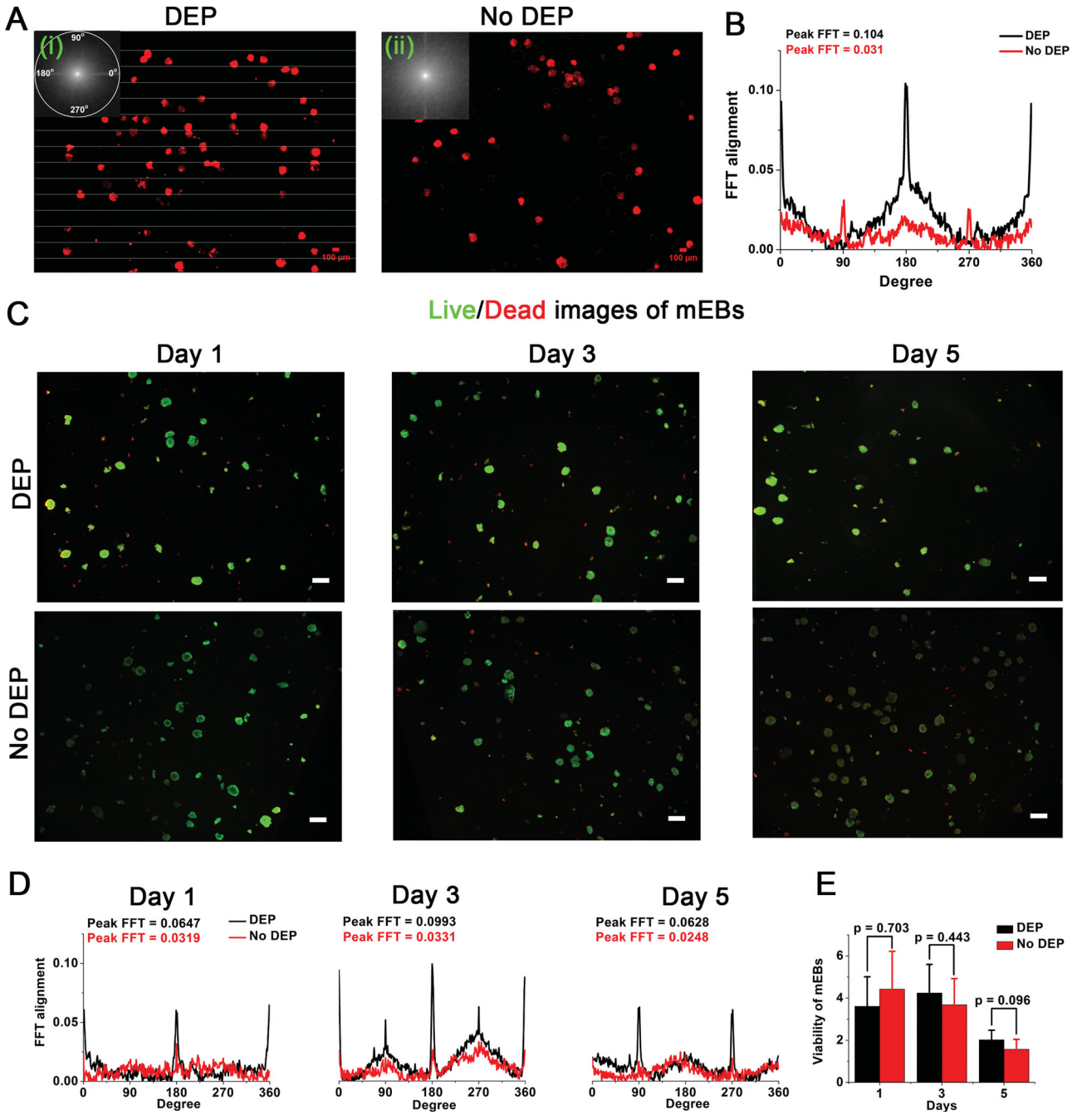

Figure 4. Alignment of C2C12 spheroids and mEBs in different hydrogels. (A) Alignment of 500 cell C2C12 spheroids in 15% PEGDA 700 labeled with red colored cell tracker dye. (i) Sample subjected to DEP. Approximate location of the electrodes is shown in the figure to show that the spheroids get pulled to the edges of the electrode, a hallmark of pDEP. (ii) No DEP sample. The inset of the plot shows the FFT of the corresponding images (Scale bar = 100 μm). (B) FFT alignment plot obtained from the FFT of the images. The alignment plot shows that the hydrogel sample subjected to DEP shows a net alignment. (C) Live/dead images of 500 cell mEBs in 15% PEGDA 3400 for days 1, 3 and 5 for both DEP and no DEP samples (Scale bar = 250 μm). (D) FFT alignment plots of the images in (C). The alignment plot shows that the hydrogel sample subjected to DEP shows a net alignment. (E) Viability of mEBs in the hydrogels ($n \geq 3$). An integrated density of 1 or higher means that there are more live cells than dead cells. There is no statistical difference in the viability of the mEBs for the DEP and the no DEP samples at $p < 0.05$.

DEP and the no DEP sample show viability of over 1, indicating that there are more live cells than dead cells. Hence, the platform can be used for patterning mEBs in 3D hydrogels while maintaining their viability.

3. Conclusion

In conclusion, we showed the patterning and encapsulation of mESCs, C2C12 cells and their spheroids in different types

of hydrogels and confirmed their viability after DEP. mESCs have the potential to differentiate into cells of the three germ layers–ectoderm, mesoderm and endoderm. However, controlling their differentiation to a particular lineage with high purity is extremely difficult because of the unknown cellular interactions with each other and their environment. DEP allows us to spatially organize the cells and their spheroids. Thus previously unknown cellular interactions can now be studied in a high throughput fashion. SL apparatus offers multi-cell, multi-material fabrication and allows for fabrication of a variety of physiologically relevant photolabile hydrogels. This combined platform thus takes us one step closer to mimicking the in vivo cellular micro-environment and can have applications in tissue engineering, regenerative medicine and stem cell differentiation.

4. Experimental Section

Cell culture: Murine-derived muscle cell line (C2C12 cells), was purchased from American Type Culture Collection (ATCC, Manassas, VA) and was cultured in Dulbecco's modified Eagle's medium (DMEM, Mediatech, Manassas, VA) supplemented with 10% fetal bovine serum (FBS, Atlanta Biologicals, Lawrenceville, GA) and 1% penicillin-streptomycin (Invitrogen, Carlsbad, CA) in standard cell culture conditions. W4129S6 mESCs (Taconic, Hudson, NY) were cultured in high glucose DMEM (Invitrogen, Carlsbad, CA) supplemented with 15% FBS, 1% penicillin-streptomycin, 1 mM sodium pyruvate, 2 mM glutamine, 100 µM non-essential amino acids, 10 ng ml^{-1} of mouse Leukemia Inhibitory Factor (mLIF) and 100 µM of mono-thiogycerol (Sigma, St. Louis, MO) on 0.1% gelatin coated petri dishes in standard cell culture conditions. Unless otherwise mentioned, all products for the culture of mESCs were purchased from Stem Cell Technologies, Vancouver, BC, Canada.

Cell patterning in the polymer mixture and hydrogel fabrication: PEGDA 700 (Sigma, St. Louis, MO) and PEGDA 3400 (Laysan Bio, Arab, AL) polymers were mixed with 0.5% 4-(2-hydroxyethoxy) phenyl-(2-hydroxy-2-propyl) ketone (Irgacure 2959, Ciba) in a LCM. 10mM HEPES (Mediatech, Manassas, VA), 100 nM $CaCl_2$ (Sigma, St. Louis, MO), 59 mM D-glucose (Sigma, St. Louis, MO) and 236 mM sucrose (Sigma, St. Louis, MO) were mixed in DI water to make the LCM.[29] Three parts of the polymer was added to one part of the cell mixture such that the final concentration of the cell-polymer solution was 10%, 15% and 20% respectively. 50 - 200 µL of this polymer-cell mixture was pipetted on the glass slide with gold (Au) micro-electrodes and was sandwiched by 18 × 18 mm coverslip. The waveform generator (Agilent, Santa Clara, CA) was turned on to provide 10 V_{pp}, 1-10 MHz sinusoid to achieve cell patterning. After the patterning, SL apparatus was used to polymerize the cell-polymer mixture to form the hydrogel.

Immunofluorescene microscopy and viability testing: In order to track the cells in the hydrogels after patterning and encapsulation, the cells were incubated with 1/1000 of cell tracker dyes (green or red, (Invitrogen, Carlsbad, CA)) before mixing it with the polymer. Viability testing was done by employing the live/dead (Invitrogen, Carlsbad, CA) assay. The cells were incubated with 2 µM calcein AM (green, live) and 4 µM of ethidium homodimer (red, dead) for 15 minutes in phenol free DMEM. After 15 minutes, the hydrogels were washed twice in phosphate buffered saline (PBS, Invitrogen, Carlsbad, CA) and immediately used for imaging. Green indicates that the cells are viable while red shows dead cells. ImageJ was used for counting the cells by taking their images in the respective channels. In order to check the viability of mEBs, the integrated density of EBs in the FITC (green, live) and the TRITC (red, dead) channel was found. The ratio of integrated density in the FITC to TRITC channel was reported as the viability of mEBs.

Characterization of the DEP solution: The electrical conductivity of the different medium used for patterning the cells/spheroids of cells was measured by using an Orion 4 star conductivity meter (Thermo Electron Corporation, Waltham, MA). The viscosity of the solution was measured by using a DV II Pro Plus viscometer (Brookfield Engineering Laboratories, Middleboro, MA).

Statistical analysis: Statistical analysis was performed using two sample t-test in OriginPro 8.5. All data values reported in the study are mean ± standard deviation (SD).

Supporting Information

Supporting Information is available from the Wiley Online Library or from the author.

Acknowledgements

The authors would like to thank Dr. Kidong Park, Dr. Bobby Reddy Jr., and Mitchell Collens for useful discussions about DEP and SLA. The authors would also like to express their gratitude towards Dr. Fei Wang for providing the mESCs and Dr. Todd McDevitt for assistance with EB formation. This project was made possible by a cooperative agreement that was awarded and administered by the U.S. Army Medical Research & Materiel Command (USAMRMC) and the Telemedicine & Advanced Technology Research Center (TATRC), under Contract #: W81XWH0810701 and National Science Foundation Science Technology Center "Emergent Behaviors of Integrated Cellular Systems" Grant CBET-0939511.

Received: September 5, 2012
Revised: November 3, 2012
Published online:

[1] D. E. Discher, P. Janmey, Y. L. Wang, *Science* **2005**, *310*, 1139.
[2] A. J. Engler, S. Sen, H. L. Sweeney, D. E. Discher, *Cell* **2006**, *126*, 677.
[3] D. E. Discher, D. J. Mooney, P. W. Zandstra, *Science* **2009**, *324*, 1673.
[4] R. McBeath, D. M. Pirone, C. M. Nelson, K. Bhadriraju, C. S. Chen, *Dev. Cell* **2004**, *6*, 483.
[5] C. S. Chen, M. Mrksich, S. Huang, G. M. Whitesides, D. E. Ingber, *Science* **1997**, *276*, 1425.
[6] S. A. Ruiz, C. S. Chen, *Stem Cells* **2008**, *26*, 2921.
[7] L. G. Griffith, M. A. Swartz, *Nat. Rev. Mol. Cell Biol.* **2006**, *7*, 211.
[8] P. Bajaj, D. Khang, T. J. Webster, *Int. J. Nanomed.* **2006**, *1*, 361.
[9] X. Tang, P. Bajaj, R. Bashir, T. A. Saif, *Soft Matter* **2011**, *7*, 6151.
[10] P. Bajaj, X. Tang, T. A. Saif, R. Bashir, *J. Biomed. Mater. Res. A* **2010**, *95A*, 1261.
[11] Y. Xu, Y. Shi, S. Ding, *Nature* **2008**, *453*, 338.
[12] S. V. Vinogradov, T. K. Bronich, A. V. Kabanov, *Adv. Drug Deliver. Rev.* **2002**, *54*, 135.
[13] T. A. Holland, J. K. V. Tessmar, Y. Tabata, A. G. Mikos, *J. Control. Release* **2004**, *94*, 101.
[14] J. L. Ifkovits, J. A. Burdick, *Tissue Eng.* **2007**, *13*, 2369.
[15] L. E. Freed, G. C. Engelmayr, J. T. Borenstein, F. T. Moutos, F. Guilak, *Adv. Mater.* **2009**, *21*, 3410.
[16] Z. G. Tang, R. A. Black, J. M. Curran, J. A. Hunt, N. P. Rhodes, D. F. Williams, *Biomaterials* **2004**, *25*, 4741.
[17] P. Basile, T. Dadali, J. Jacobson, S. Hasslund, M. Ulrich-Vinther, K. Soballe, Y. Nishio, M. H. Drissi, H. N. Langstein, D. J. Mitten, R. J. O'Keefe, E. M. Schwarz, H. A. Awad, *Mol. Ther.* **2008**, *16*, 466.
[18] L. D. Harris, B.-S. Kim, D. J. Mooney, *J. Biomed. Mater. Res.* **1998**, *42*, 396.
[19] T. J. Sill, H. A. von Recum, *Biomaterials* **2008**, *29*, 1989.

[20] V. Chan, P. Zorlutuna, J. H. Jeong, H. Kong, R. Bashir, *Lab Chip* **2010**, *10*, 2062.
[21] P. Zorlutuna, J. H. Jeong, H. Kong, R. Bashir, *Adv. Funct. Mater.* **2011**, *21*, 3642.
[22] F. P. W. Melchels, J. Feijen, D. W. Grijpma, *Biomaterials* **2010**, *31*, 6121.
[23] F. P. W. Melchels, J. Feijen, D. W. Grijpma, *Biomaterials* **2009**, *30*, 3801.
[24] H. Glasser, G. Fuhr, *Bioelectroch. Bioener.* **1998**, *47*, 301.
[25] R. Z. Lin, C. T. Ho, C. H. Liu, H. Y. Chang, *Biotechnol. J.* **2006**, *1*, 949.
[26] D. R. Albrecht, V. L. Tsang, R. L. Sah, S. N. Bhatia, *Lab Chip* **2005**, *5*, 111.
[27] D. R. Albrecht, G. H. Underhill, A. Mendelson, S. N. Bhatia, *Lab Chip* **2007**, *7*, 702.
[28] D. R. Albrecht, G. H. Underhill, T. B. Wassermann, R. L. Sah, S. N. Bhatia, *Nat. Methods* **2006**, *3*, 369.
[29] J. R. Azcon, S. Ahadian, R. Obregon, G. Camci-Unal, S. Ostrovidov, V. Hosseini, H. Kaji, K. Ino, H. Shiku, A. Khademhosseini, T. Matsue, *Lab Chip* **2012**, *12*, 2959.
[30] Y. S. Hwang, B. G. Chung, D. Ortmann, N. Hattori, H. C. Moeller, A. Khademhosseini, *Proc. Natl. Acad. Sci. USA* **2009**, *106*, 16978.
[31] D. R. Albrecht, R. L. Sah, S. N. Bhatia, *Biophys. J.* **2004**, *87*, 2131.
[32] S. V. Puttaswamy, S. Sivashankar, R. Chen, C. K. Chin, H. Y. Chang, C. H. Liu, *Biotechnol. J.* **2010**, *5*, 1005.
[33] J. P. Mazzoccoli, D. L. Feke, H. Baskaran, P. N. Pintauro, *J. Biomed. Mater. Res. A* **2010**, *93A*, 558.
[34] C. Grosse, H. P. Schwan, *Biophys. J.* **1992**, *63*, 1632.
[35] P. Ellappan, R. Sundararajan, *J. Electrostat.* **2005**, *63*, 297.
[36] W. Lee, N.J. Cho, A. Xiong, J. S. Glenn, C. W. Frank, *Proc. Natl. Acad. Sci. USA* **2010**, *107*, 20709.
[37] F. Soncin, L. Mohamet, D. Eckardt, S. Ritson, A. M. Eastham, N. Bobola, A. Russell, S. Davies, R. Kemler, C. L. R. Merry, C. M. Ward, *Stem Cells* **2009**, *27*, 2069.
[38] R. Passier, D. W. Oostwaard, J. Snapper, J. Kloots, R. J. Hassink, E. Kuijk, B. Roelen, A. B. de la Riviere, C. Mummery, *Stem Cells* **2005**, *23*, 772.
[39] A. Soto Gutierrez, N. Navarro Alvarez, D. Zhao, J. D. Rivas-Carrillo, J. Lebkowski, N. Tanaka, I. J. Fox, N. Kobayashi, *Nat. Protoc.* **2007**, *2*, 347.
[40] P. Bajaj, B. Reddy, L. Millet, C. Wei, P. Zorlutuna, G. Bao, R. Bashir, *Integr. Biol.* **2011**, *3*, 897.
[41] C. E. Ayres, G. L. Bowlin, S. C. Henderson, L. Taylor, J. Shultz, J. Alexander, T. A. Telemeco, D. G. Simpson, *Biomaterials* **2006**, *27*, 5524.
[42] C. E. Ayres, B. S. Jha, H. Meredith, J. R. Bowman, G. L. Bowlin, S. C. Henderson, D. G. Simpson, *J. Biomater. Sci. Polymer Edn.* **2008**, *19*, 603.
[43] C. E. Ayres, G. L. Bowlin, R. Pizinger, L. T. Taylor, C. A. Keen, D. G. Simpson, *Acta Biomater.* **2007**, *3*, 651.